10.6 Sea Level Change in the 21st Century

10.6.1 Global Average Sea Level Rise Due to Thermal Expansion

As seawater warms up, it expands, increasing the volume of the global ocean and producing thermosteric sea level rise (see Section 5.5.3). Global average thermal expansion can be calculated directly from simulated changes in ocean temperature. Results are available from 17 AOGCMs for the 21st century for SRES scenarios A1B, A2 and B1 (Figure 10.31), continuing from simulations of the 20th century. One ensemble member was used for each model and scenario. The time series are rather smooth compared with global average temperature time series, because thermal expansion reflects heat storage in the entire ocean, being approximately proportional to the time integral of temperature change (Gregory et al., 2001).

During 2000 to 2020 under scenario SRES A1B in the ensemble of AOGCMs, the rate of thermal expansion is 1.3 ± 0.7 mm yr^{-1}, and is not significantly different under A2 or B1. This rate is more than twice the observationally derived rate of 0.42 ± 0.12 mm yr^{-1} during 1961 to 2003. It is similar to the rate of 1.6 ± 0.5 mm yr^{-1} during 1993 to 2003 (see Section 5.5.3), which may be larger than that of previous decades partly because of natural forcing and internal variability (see Sections 5.5.2.4, 5.5.3 and 9.5.2). In particular, many of the AOGCM experiments do not include the influence of Mt. Pinatubo, the omission of which may reduce the projected rate of thermal expansion during the early 21st century.

During 2080 to 2100, the rate of thermal expansion is projected to be 1.9 ± 1.0, 2.9 ± 1.4 and 3.8 ± 1.3 mm yr^{-1} under scenarios SRES B1, A1B and A2 respectively in the AOGCM ensemble (the width of the range is affected by the different numbers of models under each scenario). The acceleration is caused by the increased climatic warming. Results are shown for all SRES marker scenarios in Table 10.7 (see Appendix 10.A for methods). In the AOGCM ensemble, under any given SRES scenario, there is some correlation of the global average temperature change across models with thermal expansion and its rate of change, suggesting that the spread in thermal expansion for that scenario is caused both by the spread in surface warming and by model-dependent ocean heat uptake efficiency (Raper et al., 2002; Table 8.2) and the distribution of added heat within the ocean (Russell et al., 2000).

10.6.2 Local Sea Level Change Due to Change in Ocean Density and Dynamics

The geographical pattern of mean sea level relative to the geoid (the dynamic topography) is an aspect of the dynamical balance relating the ocean's density structure and its circulation, which are maintained by air-sea fluxes of heat, freshwater and momentum. Over much of the ocean on multi-annual time scales, a good approximation to the pattern of dynamic topography change is given by the steric sea level change, which can be calculated straightforwardly from local temperature and salinity change (Gregory et al., 2001; Lowe and Gregory, 2006). In much of the world, salinity changes are as important as temperature changes in determining the pattern of dynamic topography change in the future, and their contributions can be opposed (Landerer et al., 2007; and as in the past, Section 5.5.4.1). Lowe and Gregory (2006) show that in the UKMO-HadCM3 AOGCM, changes in heat fluxes are the cause of many of the large-scale features of sea level change, but freshwater

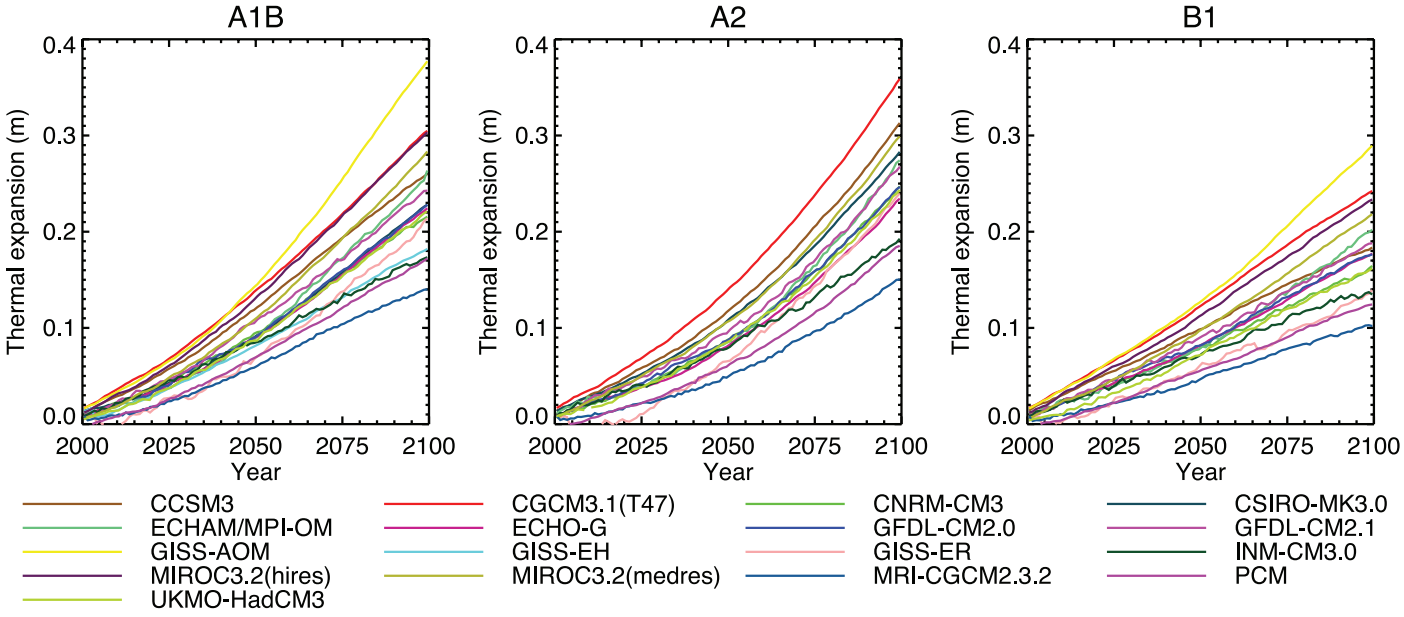

Figure 10.31. *Projected global average sea level rise (m) due to thermal expansion during the 21st century relative to 1980 to 1999 under SRES scenarios A1B, A2 and B1. See Table 8.1 for model descriptions.*

flux change dominates the North Atlantic and momentum flux change has a signature in the north and low-latitude Pacific and the Southern Ocean.

Results are available for local sea level change due to ocean density and circulation change from AOGCMs in the multi-model ensemble for the 20th century and the 21st century. There is substantial spatial variability in all models (i.e., sea level change is not uniform), and as the geographical pattern of climate change intensifies, the spatial standard deviation of local sea level change increases (Church et al., 2001; Gregory et al., 2001). Suzuki et al. (2005) show that, in their high-resolution model, enhanced eddy activity contributes to this increase, but across models there is no significant correlation of the spatial standard deviation with model spatial resolution. This section evaluates sea level change between 1980 to 1999 and 2080 to 2099 projected by 16 models forced with SRES scenario A1B. (Other scenarios are qualitatively similar, but fewer models are available.) The ratio of spatial standard deviation to global average thermal expansion varies among models, but is mostly within the range 0.3 to 0.4. The model median spatial standard deviation of thermal expansion is 0.08 m, which is about 25% of the central estimate of global average sea level rise during the 21st century under A1B (Table 10.7).

The geographical patterns of sea level change from different models are not generally similar in detail, although they have more similarity than those analysed in the TAR by Church et al. (2001). The largest spatial correlation coefficient between any pair is 0.75, but only 25% of correlation coefficients exceed 0.5. To identify common features, an ensemble mean (Figure 10.32) is examined. There are only limited areas where the model ensemble mean change exceeds the inter-model standard deviation, unlike for surface air temperature change (Section 10.3.2.1).

Like Church et al. (2001) and Gregory et al. (2001), Figure 10.32 shows smaller than average sea level rise in the Southern Ocean and larger than average in the Arctic, the former possibly due to wind stress change (Landerer et al., 2007) or low thermal expansivity (Lowe and Gregory, 2006) and the latter due to freshening. Another obvious feature is a narrow band of pronounced sea level rise stretching across the southern Atlantic and Indian Oceans and discernible in the southern Pacific. This could be associated with a southward shift in the circumpolar front (Suzuki et al., 2005) or subduction of warm anomalies in the region of formation of sub antarctic mode water (Banks et al., 2002). In the zonal mean, there are maxima of sea level rise in 30°S to 45°S and 30°N to 45°N. Similar indications are present in the altimetric and thermosteric patterns of sea level change for 1993 to 2003 (Figure 5.15). The model projections do not share other aspects of the observed pattern of sea level rise, such as in the western Pacific, which could be related to interannual variability.

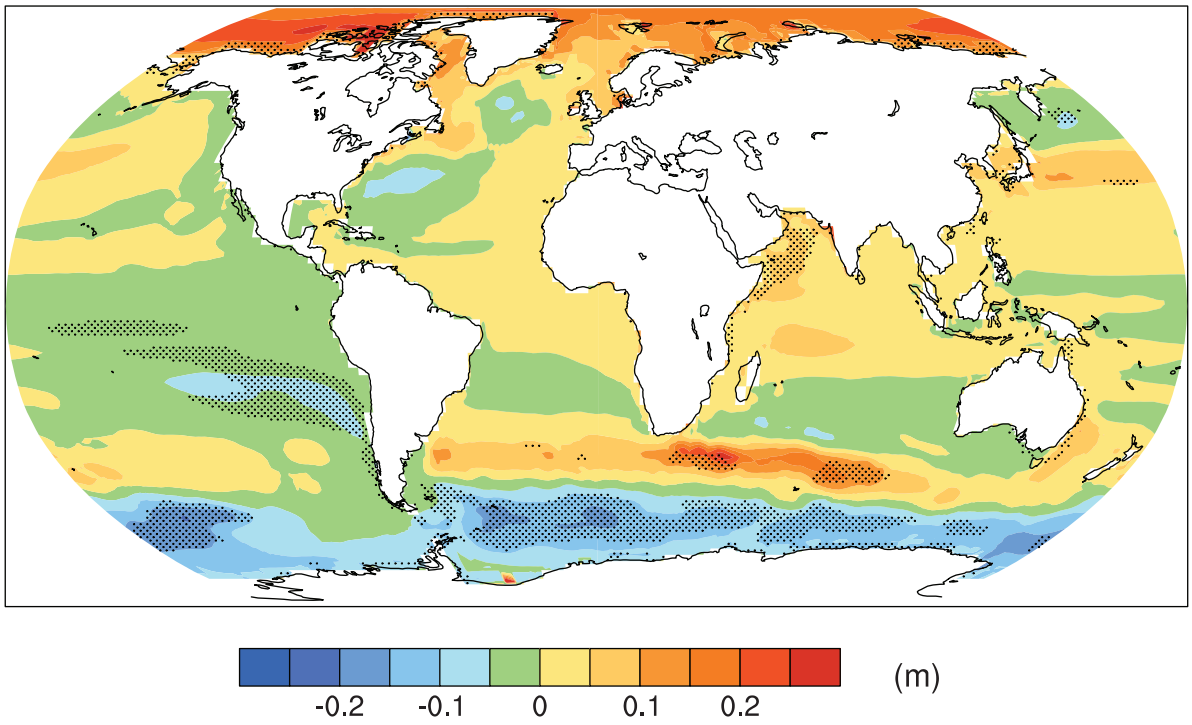

Figure 10.32. *Local sea level change (m) due to ocean density and circulation change relative to the global average (i.e., positive values indicate greater local sea level change than global) during the 21st century, calculated as the difference between averages for 2080 to 2099 and 1980 to 1999, as an ensemble mean over 16 AOGCMs forced with the SRES A1B scenario. Stippling denotes regions where the magnitude of the multi-model ensemble mean divided by the multi-model standard deviation exceeds 1.0.*

The North Atlantic dipole pattern noted by Church et al. (2001), that is, reduced rise to the south of the Gulf Stream extension, enhanced to the north, consistent with a weakening of the circulation, is present in some models; a more complex feature is described by Landerer et al. (2007). The reverse is apparent in the north Pacific, which Suzuki et al. (2005) associate with a wind-driven intensification of the Kuroshio Current. Using simplified models, Hsieh and Bryan (1996) and Johnson and Marshall (2002) show how upper-ocean velocities and sea level would be affected in North Atlantic coastal regions within months of a cessation of sinking in the North Atlantic as a result of propagation by coastal and equatorial Kelvin waves, but would take decades to adjust in the central regions and the south Atlantic. Levermann et al. (2005) show that a sea level rise of several tenths of a metre could be realised in coastal regions of the North Atlantic within a few decades (i.e., tens of millimetres per year) of a collapse of the MOC. Such changes to dynamic topography would be much more rapid than global average sea level change. However, it should be emphasized that these studies are sensitivity tests, not projections; the Atlantic MOC does not collapse in the SRES scenario runs evaluated here (see Section 10.3.4).

The geographical pattern of sea level change is affected also by changes in atmospheric surface pressure, but this is a relatively small effect given the projected pressure changes (Figure 10.9; a pressure increase of 1 hPa causes a drop in local sea level of 0.01 m; see Section 5.5.4.3). Land movements and changes in the gravitational field resulting from the changing loading of the crust by water and ice also have effects which are small over most of the ocean (see Section 5.5.4.4).

10.6.3 Glaciers and Ice Caps

Glaciers and ice caps (G&IC, see also Section 4.5.1) comprise all land ice except for the ice sheets of Greenland and Antarctica (see Sections 4.6.1 and 10.6.4). The mass of G&IC can change because of changes in surface mass balance (Section 10.6.3.1). Changes in mass balance cause changes in area and thickness (Section 10.6.3.2), with feedbacks on surface mass balance.

10.6.3.1 Mass Balance Sensitivity to Temperature and Precipitation

Since G&IC mass balance depends strongly on their altitude and aspect, use of data from climate models to make projections requires a method of downscaling, because individual G&IC are much smaller than typical AOGCM grid boxes. Statistical relations for meteorological quantities can be developed between the GCM and local scales (Reichert et al., 2002), but they may not continue to hold in future climates. Hence, for projections the approach usually adopted is to use GCM simulations of changes in climate parameters to perturb the observed climatology or mass balance (Gregory and Oerlemans, 1998; Schneeberger et al., 2003).

Change in ablation (mostly melting) of a glacier or ice cap is modelled using b_T (in m yr^{-1} °C^{-1}), the sensitivity of the mean specific surface mass balance to temperature (refer to Section 4.5 for a discussion of the relation of mass balance to climate). One approach determines b_T by energy balance modelling, including evolution of albedo and refreezing of melt water within the firn (Zuo and Oerlemans, 1997). Oerlemans and Reichert (2000), Oerlemans (2001) and Oerlemans et al. (2006) refine this approach to include dependence on monthly temperature and precipitation changes. Another approach uses a degree-day method, in which ablation is proportional to the integral of mean daily temperature above the freezing point (Braithwaite et al., 2003). Braithwaite and Raper (2002) show that there is excellent consistency between the two approaches, which indicates a similar relationship between b_T and climatological precipitation. Schneeberger et al. (2000, 2003) use a degree-day method for ablation modified to include incident solar radiation, again obtaining similar results. De Woul and Hock (2006) find somewhat larger sensitivities for arctic G&IC from the degree-day method than the energy balance method. Calculations of b_T are estimated to have an uncertainty of ±15% (standard deviation) (Gregory and Oerlemans, 1998; Raper and Braithwaite, 2006).

The global average sensitivity of G&IC surface mass balance to temperature is estimated by weighting the local sensitivities by land ice area in various regions. For a geographically and seasonally uniform rise in global temperature, Oerlemans and Fortuin (1992) derive a global average G&IC surface mass balance sensitivity of –0.40 m yr^{-1} °C^{-1}, Dyurgerov and Meier (2000) –0.37 m yr^{-1} °C^{-1} (from observations), Braithwaite and Raper (2002) –0.41 m yr^{-1} °C^{-1} and Raper and Braithwaite (2005) –0.35 m yr^{-1} °C^{-1}. Applying the scheme of Oerlemans (2001) and Oerlemans et al. (2006) worldwide gives a smaller value of –0.32 m yr^{-1} °C^{-1}, the reduction being due to the modified treatment of albedo by Oerlemans (2001).

These global average sensitivities for uniform temperature change are given only for scenario-independent comparison of the various methods; they cannot be used for projections, which require regional and seasonal temperature changes (Gregory and Oerlemans, 1998; van de Wal and Wild, 2001). Using monthly temperature changes simulated in G&IC regions by 17 AR4 AOGCMs for scenarios A1B, A2 and B1, the global total surface mass balance sensitivity to global average temperature change for all G&IC outside Greenland and Antarctica is 0.61 ± 0.12 mm yr^{-1} °C^{-1} (sea level equivalent) with the b_T of Zuo and Oerlemans (1997) or 0.49 ± 0.13 mm yr^{-1} °C^{-1} with those of Oerlemans (2001) and Oerlemans et al. (2006), subject to uncertainty in G&IC area (see Section 4.5.2 and Table 4.4).

Hansen and Nazarenko (2004) collate measurements of soot (fossil fuel black carbon) in snow and estimate consequent reductions in snow and ice albedo of between 0.001 for the pristine conditions of Antarctica and over 0.10 for polluted NH land areas. They argue that glacial ablation would be increased by this effect. While it is true that soot has not been explicitly considered in existing sensitivity estimates, it may already be included because the albedo and degree-day parametrizations have been empirically derived from data collected in affected regions.

For seasonally uniform temperature rise, Oerlemans et al. (1998) find that an increase in precipitation of 20 to 50% °C^{-1} is required to balance increased ablation, while Braithwaite et al. (2003) report a required precipitation increase of 29 to 41% °C^{-1}, in both cases for a sample of G&IC representing a variety of climatic regimes. Oerlemans et al. (2006) require a precipitation increase of 20 to 43% °C^{-1} to balance ablation increase, and de Woul and Hock (2006) approximately 20% °C^{-1} for Arctic G&IC. Although AOGCMs generally project larger than average precipitation change in northern mid- and high-latitude regions, the global average is 1 to 2% °C^{-1} (Section 10.3.1), so ablation increases would be expected to dominate worldwide. However, precipitation changes may sometimes dominate locally (see Section 4.5.3).

Regressing observed global total mass balance changes of all G&IC outside Greenland and Antarctica against global average surface temperature change gives a global total mass balance sensitivity which is greater than model results (see Appendix 10.A). The current state of knowledge does not permit a satisfactory explanation of the difference. Giving more weight to the observational record but enlarging the uncertainty to allow for systematic error, a value of 0.80 ± 0.33 mm yr^{-1} °C^{-1} (5 to 95% range) is adopted for projections. The regression indicates that the climate of 1865 to 1895 was 0.13°C warmer globally than the climate that gives a steady state for G&IC (cf., Zuo and Oerlemans, 1997; Gregory et al., 2006). Model results for the 20th century are sensitive to this value, but the projected temperature change in the 21st century is large by comparison, making the effect relatively less important for projections (see Appendix 10.A).

10.6.3.2 Dynamic Response and Feedback on Mass Balance

As glacier volume is lost, glacier area declines so the ablation decreases. Oerlemans et al. (1998) calculate that omitting this effect leads to overestimates of ablation of about 25% by 2100. Church et al. (2001), following Bahr et al. (1997) and Van de Wal and Wild (2001), make some allowance for it by diminishing the area A of a glacier of volume V according to $V \propto A^{1.375}$. This is a scaling relation derived for glaciers in a steady state, which may hold only approximately during retreat. For example, thinning in the ablation zone will steepen the surface slope and tend to increase the flow. Comparison with a simple flow model suggests the deviations do not exceed 20% (van de Wal and Wild, 2001). Schneeberger et al. (2003) find that the scaling relation produced a mixture of over- and underestimates of volume loss for their sample of glaciers compared with more detailed dynamic modelling. In some regions where G&IC flow into the sea or lakes there is accelerated dynamic discharge (Rignot et al., 2003) that is not included in currently available glacier models, leading to an underestimate of G&IC mass loss.

The mean specific surface mass balance of the glacier or ice cap will change as volume is lost: lowering the ice surface as the ice thins will tend to make it more negative, but the predominant loss of area at lower altitude in the ablation zone will tend to make it less negative (Braithwaite and Raper, 2002). For rapid thinning rates in the ablation zone, of several metres per year, lowering the surface will give enhanced local warmings comparable to the rate of projected climatic warming. However, those areas of the ablation zone of valley glaciers that thin most rapidly will soon be removed altogether, resulting in retreat of the glacier. The enhancement of ablation by surface lowering can only be sustained in glaciers with a relatively large, thick and flat ablation area. On multi-decadal time scales, for the majority of G&IC, the loss of area is more important than lowering of the surface (Schneeberger et al., 2003).

The dynamical approach (Oerlemans et al., 1998; Schneeberger et al., 2003) cannot be applied to all the world's glaciers individually as the required data are unknown for the vast majority of them. Instead, it might be applied to a representative ensemble derived from statistics of size distributions of G&IC. Raper et al. (2000) developed a geometrical approach, in which the width, thickness and length of a glacier are reduced as its volume and area declines. When applied statistically to the world population of glaciers and individually to ice caps, this approach shows that the reduction of area of glaciers strongly reduces the ablation during the 21st century (Raper and Braithwaite, 2006), by about 45% under scenario SRES A1B for the GFDL-CM2.0 and PCM AOGCMs (see Table 8.1 for model details). For the same cases, using the mass-balance sensitivities to temperature of Oerlemans (2001) and Oerlemans et al. (2006), G&IC mass loss is reduced by about 35% following the area scaling of Van de Wal and Wild (2001), suggesting that the area scaling and the geometrical model have a similar effect in reducing estimated ablation for the 21st century. The effect is greater when using the observationally derived mass balance sensitivity (Section 10.6.3.1), which is larger, implying faster mass loss for fixed area. The uncertainty in present-day glacier volume (Table 4.4) introduces a 5 to 10% uncertainty into the results of area scaling. For projections, the area scaling of Van de Wal and Wild (2001) is applied, using three estimates of world glacier volume (see Table 4.4 and Appendix 10.A). The scaling reduces the projections of the G&IC contribution up to the mid-21st century by 25% and over the whole century by 40 to 50% with respect to fixed G&IC area.

10.6.3.3 Glaciers and Ice Caps on Greenland and Antarctica

The G&IC on Greenland and Antarctica (apart from the ice sheets) have been less studied and projections for them are consequently more uncertain. A model estimate for the G&IC on Greenland indicates an addition of about 6% to the G&IC sea level contribution in the 21st century (van de Wal and Wild, 2001). Using a degree-day scheme, Vaughan (2006) estimates that ablation of glaciers in the Antarctic Peninsula presently amounts to 0.008 to 0.055 mm yr^{-1} of sea level, 1 to 9% of the contribution from G&IC outside Greenland and Antarctica (Table 4.4). Morris and Mulvaney (2004) find that accumulation increases on the Antarctic Peninsula were larger than ablation increases during 1972 to 1998, giving a small net *negative* sea

level contribution from the region. However, because ablation increases nonlinearly with temperature, they estimate that for future warming the contribution would become positive, with a sensitivity of 0.07 ± 0.03 mm yr^{-1} $°C^{-1}$ to uniform temperature change in Antarctica, that is, about 10% of the global sensitivity of G&IC outside Greenland and Antarctica (Section 10.6.3.1).

These results suggest that the Antarctic and Greenland G&IC will together give 10 to 20% of the sea level contribution of other G&IC in future decades. In recent decades, the G&IC on Greenland and Antarctica have together made a contribution of about 20% of the total of other G&IC (see Section 4.5.2). On these grounds, the global G&IC sea level contribution is increased by a factor of 1.2 to include those in Greenland and Antarctica in projections for the 21st century (see Section 10.6.5 and Table 10.7). Dynamical acceleration of glaciers in Greenland and Antarctica following removal of ice shelves, as has recently happened on the Antarctic Peninsula (Sections 4.6.2.2 and 10.6.4.2), would add further to this, and is included in projections of that effect (Section 10.6.4.3).

10.6.4 Ice Sheets

The mass of ice grounded on land in the Greenland and Antarctic Ice Sheets (see also Section 4.6.1) can change as a result of changes in surface mass balance (the sum of accumulation and ablation; Section 10.6.4.1) or in the flux of ice crossing the grounding line, which is determined by the dynamics of the ice sheet (Section 10.6.4.2). Surface mass balance and dynamics together both determine and are affected by the change in surface topography.

10.6.4.1 Surface Mass Balance

Surface mass balance (SMB) is immediately influenced by climate change. A good simulation of the ice sheet SMB requires a resolution exceeding that of AGCMs used for long climate experiments, because of the steep slopes at the margins of the ice sheet, where the majority of the precipitation and all of the ablation occur. Precipitation over ice sheets is typically overestimated by AGCMs, because their smooth topography does not present a sufficient barrier to inland penetration (Ohmura et al., 1996; Glover, 1999; Murphy et al., 2002). Ablation also tends to be overestimated because the area at low altitude around the margins of the ice sheet, where melting preferentially occurs, is exaggerated (Glover, 1999; Wild et al., 2003). In addition, AGCMs do not generally have a representation of the refreezing of surface melt water within the snowpack and may not include albedo variations dependent on snow ageing and its conversion to ice.

To address these issues, several groups have computed SMB at resolutions of tens of kilometres or less, with results that compare acceptably well with observations (e.g., van Lipzig et al., 2002; Wild et al., 2003). Ablation is calculated either by schemes based on temperature (degree-day or other temperature index methods) or by energy balance modelling. In the studies listed in Table 10.6, changes in SMB have been calculated from climate change simulations with high-resolution AGCMs or by perturbing a high-resolution observational climatology with climate model output, rather than by direct use of low-resolution GCM results. The models used for projected SMB changes are similar in kind to those used to study recent SMB changes (Section 4.6.3.1).

All the models show an increase in accumulation, but there is considerable uncertainty in its size (Table 10.6; van de Wal et al., 2001; Huybrechts et al., 2004). Precipitation increase could be determined by atmospheric radiative balance, increase in saturation specific humidity with temperature, circulation changes, retreat of sea ice permitting greater evaporation or a combination of these (van Lipzig et al., 2002). Accumulation also depends on change in local temperature, which strongly affects whether precipitation is solid or liquid (Janssens and Huybrechts, 2000), tending to make the accumulation increase smaller than the precipitation increase for a given temperature rise. For Antarctica, accumulation increases by 6 to 9% $°C^{-1}$ in the high-resolution AGCMs. Precipitation increases somewhat less in AR4 AOGCMs (typically of lower resolution), by 3 to 8% $°C^{-1}$. For Greenland, accumulation derived from the high-resolution AGCMs increases by 5 to 9% $°C^{-1}$. Precipitation increases by 4 to 7% $°C^{-1}$ in the AR4 AOGCMs.

Kapsner et al. (1995) do not find a relationship between precipitation and temperature variability inferred from Greenland ice cores for the Holocene, although both show large changes from the Last Glacial Maximum (LGM) to the Holocene. In the UKMO-HadCM3 AOGCM, the relationship is strong for climate change forced by greenhouse gases and the glacial-interglacial transition, but weaker for naturally forced variability (Gregory et al., 2006). Increasing precipitation in conjunction with warming has been observed in recent years in Greenland (Section 4.6.3.1).

All studies for the 21st century project that antarctic SMB changes will contribute negatively to sea level, owing to increasing accumulation exceeding any ablation increase (see Table 10.6). This tendency has not been observed in the average over Antarctica in reanalysis products for the last two decades (see Section 4.6.3.1), but during this period Antarctica as a whole has not warmed; on the other hand, precipitation has increased on the Antarctic Peninsula, where there has been strong warming.

In projections for Greenland, ablation increase is important but uncertain, being particularly sensitive to temperature change around the margins. Climate models project less warming in these low-altitude regions than the Greenland average, and less warming in summer (when ablation occurs) than the annual average, but greater warming in Greenland than the global average (Church et al., 2001; Huybrechts et al., 2004; Chylek and Lohmann, 2005; Gregory and Huybrechts, 2006). In most studies, Greenland SMB changes represent a net positive contribution to sea level in the 21st century (Table 10.6; Kiilsholm et al., 2003) because the ablation increase is larger than the precipitation increase. Only Wild et al. (2003) find the opposite, so that the net SMB change contributes negatively to sea level in the 21st century. Wild et al. (2003) attribute this

Table 10.6. *Comparison of ice sheet (grounded ice area) SMB changes calculated from high-resolution climate models. $\Delta P/\Delta T$ is the change in accumulation divided by change in temperature over the ice sheet, expressed as sea level equivalent (positive for falling sea level), and $\Delta R/\Delta T$ the corresponding quantity for ablation (positive for rising sea level). Note that ablation increases more rapidly than linearly with ΔT (van de Wal et al., 2001; Gregory and Huybrechts, 2006). To convert from mm yr^{-1} °C^{-1} to kg yr^{-1} °C^{-1}, multiply by 3.6 × 10^{14} m^2. To convert mm yr^{-1} °C^{-1} of sea level equivalent to mm yr^{-1} °C^{-1} averaged over the ice sheet, multiply by –206 for Greenland and –26 for Antarctica. $\Delta P/(P\Delta T)$ is the fractional change in accumulation divided by the change in temperature.*

Study	Climate model[a]	Model resolution and SMB source[b]	Greenland			Antarctica	
			$\Delta P/\Delta T$ (mm yr^{-1} °C^{-1})	$\Delta P/(P\Delta T)$ (% °C^{-1})	$\Delta R/\Delta T$ (mm yr^{-1} °C^{-1})	$\Delta P/\Delta T$ (mm yr^{-1} °C^{-1})	$\Delta P/(P\Delta T)$ (% °C^{-1})
Van de Wal et al. (2001)	ECHAM4	20 km EB	0.14	8.5	0.16	n.a.	n.a.
Wild and Ohmura (2000)	ECHAM4	T106 ≈ 1.1° EB	0.13	8.2	0.22	0.47	7.4
Wild et al. (2003)	ECHAM4	2 km TI	0.13	8.2	0.04	0.47	7.4
Bugnion and Stone (2002)	ECHAM4	20 km EB	0.10	6.4	0.13	n.a.	n.a.
Huybrechts et al. (2004)	ECHAM4	20 km TI	0.13[c]	7.6[c]	0.14	0.49[c]	7.3[c]
Huybrechts et al. (2004)	HadAM3H	20 km TI	0.09[c]	4.7[c]	0.23	0.37[c]	5.5[c]
Van Lipzig et al. (2002)	RACMO	55 km EB	n.a.	n.a.	n.a.	0.53	9.0
Krinner et al. (2007)	LMDZ4	60 km EB	n.a.	n.a.	n.a.	0.49	8.4

Notes:
[a] ECHAM4: Max Planck Institute for Meteorology AGCM; HadAM3H: high-resolution Met Office Hadley Centre AGCM; RACMO: Regional Atmospheric Climate Model (for Antarctica); LMDZ4: Laboratoire de Météorologie Dynamique AGCM (with high resolution over Antarctica).
[b] EB: SMB calculated from energy balance; TI: SMB calculated from temperature index.
[c] In these cases *P* is precipitation rather than accumulation.

difference to the reduced ablation area in their higher-resolution grid. A positive SMB change is not consistent with analyses of recent changes in Greenland SMB (see Section 4.6.3.1).

For an average temperature change of 3°C over each ice sheet, a combination of four high-resolution AGCM simulations and 18 AR4 AOGCMs (Huybrechts et al., 2004; Gregory and Huybrechts, 2006) gives SMB changes of 0.3 ± 0.3 mm yr^{-1} for Greenland and –0.9 ± 0.5 mm yr^{-1} for Antarctica (sea level equivalent), that is, sensitivities of 0.11 ± 0.09 mm yr^{-1} °C^{-1} for Greenland and –0.29 ± 0.18 mm yr^{-1} °C^{-1} for Antarctica. These results generally cover the range shown in Table 10.6, but tend to give more positive (Greenland) or less negative (Antarctica) sea level rise because of the smaller precipitation increases projected by the AOGCMs than by the high-resolution AGCMs. The uncertainties are from the spatial and seasonal patterns of precipitation and temperature change over the ice sheets, and from the ablation calculation. Projections under SRES scenarios for the 21st century are shown in Table 10.7.

10.6.4.2 Dynamics

Ice sheet flow reacts to changes in topography produced by SMB change. Projections for the 21st century are given in Section 10.6.5 and Table 10.7, based on the discussion in this section. In Antarctica, topographic change tends to increase ice flow and discharge. In Greenland, lowering of the surface tends to increase the ablation, while a steepening slope in the ablation zone opposes the lowering, and thinning of outlet glaciers reduces discharge. Topographic and dynamic changes simulated by ice flow models (Huybrechts and De Wolde, 1999; van de Wal et al., 2001; Huybrechts et al., 2002, 2004; Gregory and Huybrechts, 2006) can be roughly represented as modifying the sea level changes due to SMB change with fixed topography by –5% ± 5% from Antarctica, and 0% ±10% from Greenland (± one standard deviation) during the 21st century.

The TAR concluded that accelerated sea level rise caused by rapid dynamic response of the ice sheets to climate change is very unlikely during the 21st century (Church et al., 2001). However, new evidence of recent rapid changes in the Antarctic Peninsula, West Antarctica and Greenland (see Section 4.6.3.3) has again raised the possibility of larger dynamical changes in the future than are projected by state-of-the-art continental models, such as cited above, because these models do not incorporate all the processes responsible for the rapid marginal thinning currently taking place (Box 4.1; Alley et al., 2005a; Vaughan, 2007).

The main uncertainty is the degree to which the presence of ice shelves affects the flow of inland ice across the grounding

Frequently Asked Question 10.2

How Likely are Major or Abrupt Climate Changes, such as Loss of Ice Sheets or Changes in Global Ocean Circulation?

Abrupt climate changes, such as the collapse of the West Antarctic Ice Sheet, the rapid loss of the Greenland Ice Sheet or large-scale changes of ocean circulation systems, are not considered likely to occur in the 21st century, based on currently available model results. However, the occurrence of such changes becomes increasingly more likely as the perturbation of the climate system progresses.

Physical, chemical and biological analyses from Greenland ice cores, marine sediments from the North Atlantic and elsewhere and many other archives of past climate have demonstrated that local temperatures, wind regimes and water cycles can change rapidly within just a few years. The comparison of results from records in different locations of the world shows that in the past major changes of hemispheric to global extent occurred. This has led to the notion of an unstable past climate that underwent phases of abrupt change. Therefore, an important concern is that the continued growth of greenhouse gas concentrations in the atmosphere may constitute a perturbation sufficiently strong to trigger abrupt changes in the climate system. Such interference with the climate system could be considered dangerous, because it would have major global consequences.

Before discussing a few examples of such changes, it is useful to define the terms 'abrupt' and 'major'. 'Abrupt' conveys the meaning that the changes occur much faster than the perturbation inducing the change; in other words, the response is nonlinear. A 'major' climate change is one that involves changes that exceed the range of current natural variability and have a spatial extent ranging from several thousand kilometres to global. At local to regional scales, abrupt changes are a common characteristic of natural climate variability. Here, isolated, short-lived events that are more appropriately referred to as 'extreme events' are not considered, but rather large-scale changes that evolve rapidly and persist for several years to decades. For instance, the mid-1970s shift in sea surface temperatures in the Eastern Pacific, or the salinity reduction in the upper 1,000 m of the Labrador Sea since the mid-1980s, are examples of abrupt events with local to regional consequences, as opposed to the larger-scale, longer-term events that are the focus here.

One example is the potential collapse, or shut-down of the Gulf Stream, which has received broad public attention. The Gulf Stream is a primarily horizontal current in the north-western Atlantic Ocean driven by winds. Although a stable feature of the general circulation of the ocean, its northern extension, which feeds deep-water formation in the Greenland-Norwegian-Iceland Seas and thereby delivers substantial amounts of heat to these seas and nearby land areas, is influenced strongly by changes in the density of the surface waters in these areas. This current constitutes the northern end of a basin-scale meridional overturning circulation (MOC) that is established along the western boundary of the Atlantic basin. A consistent result from climate model simulations is that if the density of the surface waters in the North Atlantic decreases due to warming or a reduction in salinity, the strength of the MOC is decreased, and with it, the delivery of heat into these areas. Strong sustained reductions in salinity could induce even more substantial reduction, or complete shut-down of the MOC in all climate model projections. Such changes have indeed happened in the distant past.

The issue now is whether the increasing human influence on the atmosphere constitutes a strong enough perturbation to the MOC that such a change might be induced. The increase in greenhouse gases in the atmosphere leads to warming and an intensification of the hydrological cycle, with the latter making the surface waters in the North Atlantic less salty as increased rain leads to more freshwater runoff to the ocean from the region's rivers. Warming also causes land ice to melt, adding more freshwater and further reducing the salinity of ocean surface waters. Both effects would reduce the density of the surface waters (which must be dense and heavy enough to sink in order to drive the MOC), leading to a reduction in the MOC in the 21st century. This reduction is predicted to proceed in lockstep with the warming: none of the current models simulates an abrupt (nonlinear) reduction or a complete shut-down in this century. There is still a large spread among the models' simulated reduction in the MOC, ranging from virtually no response to a reduction of over 50% by the end of the 21st century. This cross-model variation is due to differences in the strengths of atmosphere and ocean feedbacks simulated in these models.

Uncertainty also exists about the long-term fate of the MOC. Many models show a recovery of the MOC once climate is stabilised. But some models have thresholds for the MOC, and they are passed when the forcing is strong enough and lasts long enough. Such simulations then show a gradual reduction of the MOC that continues even after climate is stabilised. A quantification of the likelihood of this occurring is not possible at this stage. Nevertheless, even if this were to occur, Europe would still experience warming, since the radiative forcing caused by increasing greenhouse gases would overwhelm the cooling associated with the MOC reduction. Catastrophic scenarios suggesting the beginning of an ice age triggered by a shutdown of the MOC are thus mere speculations, and no climate model has produced such an outcome. In fact, the processes leading to an ice age are sufficiently well understood and so completely different from those discussed here, that we can confidently exclude this scenario.

(continued)

Irrespective of the long-term evolution of the MOC, model simulations agree that the warming and resulting decline in salinity will significantly reduce deep and intermediate water formation in the Labrador Sea during the next few decades. This will alter the characteristics of the intermediate water masses in the North Atlantic and eventually affect the deep ocean. The long-term effects of such a change are unknown.

Other widely discussed examples of abrupt climate changes are the rapid disintegration of the Greenland Ice Sheet, or the sudden collapse of the West Antarctic Ice Sheet. Model simulations and observations indicate that warming in the high latitudes of the Northern Hemisphere is accelerating the melting of the Greenland Ice Sheet, and that increased snowfall due to the intensified hydrological cycle is unable to compensate for this melting. As a consequence, the Greenland Ice Sheet may shrink substantially in the coming centuries. Moreover, results suggest that there is a critical temperature threshold beyond which the Greenland Ice Sheet would be committed to disappearing completely, and that threshold could be crossed in this century. However, the total melting of the Greenland Ice Sheet, which would raise global sea level by about seven metres, is a slow process that would take many hundreds of years to complete.

Recent satellite and *in situ* observations of ice streams behind disintegrating ice shelves highlight some rapid reactions of ice sheet systems. This raises new concern about the overall stability of the West Antarctic Ice Sheet, the collapse of which would trigger another five to six metres of sea level rise. While these streams appear buttressed by the shelves in front of them, it is currently unknown whether a reduction or failure of this buttressing of relatively limited areas of the ice sheet could actually trigger a widespread discharge of many ice streams and hence a destabilisation of the entire West Antarctic Ice Sheet. Ice sheet models are only beginning to capture such small-scale dynamical processes that involve complicated interactions with the glacier bed and the ocean at the perimeter of the ice sheet. Therefore, no quantitative information is available from the current generation of ice sheet models as to the likelihood or timing of such an event.

line. A strong argument for enhanced flow when the ice shelf is removed is yielded by the acceleration of Jakobshavn Glacier (Greenland) following the loss of its floating tongue, and of the glaciers supplying the Larsen B Ice Shelf (Antarctic Peninsula) after it collapsed (see Section 4.6.3.3). The onset of disintegration of the Larsen B Ice Shelf has been attributed to enhanced fracturing by crevasses promoted by surface melt water (Scambos et al., 2000). Large portions of the Ross and Filchner-Ronne Ice Shelves (West Antarctica) currently have mean summer surface temperatures of around –5°C (Comiso, 2000, updated). Four high-resolution GCMs (Gregory and Huybrechts, 2006) project summer surface warming in these major ice shelf regions of between 0.2 and 1.3 times the antarctic annual average warming, which in turn will be a factor 1.1 ± 0.3 greater than global average warming according to AOGCM simulations using SRES scenarios. These figures indicate that a local mean summer warming of 5°C is unlikely for a global warming of less than 5°C (see Appendix 10.A). This suggests that ice shelf collapse due to surface melting is unlikely under most SRES scenarios during the 21st century, but we have low confidence in the inference because there is evidently large systematic uncertainty in the regional climate projections, and it is not known whether episodic surface melting might initiate disintegration in a warmer climate while mean summer temperatures remain below freezing.

In the Amundsen Sea sector of West Antarctica, ice shelves are not so extensive and the cause of ice shelf thinning is not surface melting, but bottom melting at the grounding line (Rignot and Jacobs, 2002). Shepherd et al. (2004) find an average ice-shelf thinning rate of 1.5 ± 0.5 m yr^{-1}. At the same time as the basal melting, accelerated inland flow has been observed for Pine Island, Thwaites and other glaciers in the sector (Rignot, 1998, 2001; Thomas et al., 2004). The synchronicity of these changes strongly implies that their cause lies in oceanographic change in the Amundsen Sea, but this has not been attributed to anthropogenic climate change and could be connected with variability in the SAM.

Because the acceleration took place in only a few years (Rignot et al., 2002; Joughin et al., 2003) but appears up to about 150 km inland, it implies that the dynamical response to changes in the ice shelf can propagate rapidly up the ice stream. This conclusion is supported by modelling studies of Pine Island Glacier by Payne et al. (2004) and Dupont and Alley (2005), in which a single and instantaneous reduction of the basal or lateral drag at the ice front is imposed in idealised ways, such as a step retreat of the grounding line. The simulated acceleration and inland thinning are rapid but transient; the rate of contribution to sea level declines as a new steady state is reached over a few decades. In the study of Payne et al. (2004) the imposed perturbations were designed to resemble loss of drag in the 'ice plain', a partially grounded region near the ice front, and produced a velocity increase of about 1 km yr^{-1} there. Thomas et al. (2005) suggest the ice plain will become ungrounded during the next decade and obtain a similar velocity increase using a simplified approach.

Most of inland ice of West Antarctica is grounded below sea level and so it could float if it thinned sufficiently; discharge therefore promotes inland retreat of the grounding line, which

represents a positive feedback by further reducing basal traction. Unlike the one-time change in the idealised studies, this would represent a sustained dynamical forcing that would prolong the contribution to sea level rise. Grounding line retreat of the ice streams has been observed recently at rates of up to about 1 km yr^{-1} (Rignot, 1998, 2001; Shepherd et al., 2002), but a numerical model formulation is difficult to construct (Vieli and Payne, 2005).

The majority of West Antarctic ice discharge is through the ice streams that feed the Ross and Ronne-Filchner ice shelves, but in these regions no accelerated flow causing thinning is currently observed; on the contrary, they are thickening or near balance (Zwally et al., 2005). Excluding these regions, and likewise those parts of the East Antarctic Ice Sheet that drain into the large Amery ice shelf, the total area of ice streams (areas flowing faster than 100 m yr^{-1}) discharging directly into the sea or via a small ice shelf is 270,000 km^2. If all these areas thinned at 2 m yr^{-1}, the order of magnitude of the larger rates observed in fast-flowing areas of the Amundsen Sea sector (Shepherd et al., 2001, 2002), the contribution to sea level rise would be about 1.5 mm yr^{-1}. This would require sustained retreat simultaneously on many fronts, and should be taken as an indicative upper limit for the 21st century (see also Section 10.6.5).

The observation in west-central Greenland of seasonal variation in ice flow rate and of a correlation with summer temperature variation (Zwally et al., 2002) suggest that surface melt water may join a sub-glacially routed drainage system lubricating the ice flow (although this implies that it penetrates more than 1,200 m of subfreezing ice). By this mechanism, increased surface melting during the 21st century could cause acceleration of ice flow and discharge; a sensitivity study (Parizek and Alley, 2004) indicated that this might increase the sea level contribution from the Greenland Ice Sheet during the 21st century by up to 0.2 m, depending on the warming and other assumptions. However, other studies (Echelmeyer and Harrison, 1990; Joughin et al., 2004) found no evidence of seasonal fluctuations in the flow rate of nearby Jakobshavn Glacier despite a substantial supply of surface melt water.

10.6.5 Projections of Global Average Sea Level Change for the 21st Century

Table 10.7 and Figure 10.33 show projected changes in global average sea level under the SRES marker scenarios for the 21st century due to thermal expansion and land ice changes based on AR4 AOGCM results (see Sections 10.6.1, 10.6.3 and 10.6.4 for discussion). The ranges given are 5 to 95% intervals characterising the spread of model results, but we are not able to assess their likelihood in the way we have done for temperature change (Section 10.5.4.6), for two main reasons. First, the observational constraint on sea level rise projections is weaker, because records are shorter and subject to more uncertainty. Second, current scientific understanding leaves poorly known uncertainties in the methods used to make projections for land ice (Sections 10.6.3 and 10.6.4). Since the AOGCMs are integrated with scenarios of CO_2 concentration, uncertainties in carbon cycle feedbacks are not included in the results. The carbon cycle uncertainty in projections of temperature change cannot be translated into sea level rise because thermal expansion is a major contributor and its relation to temperature change is uncertain (Section 10.6.1).

Table 10.7. *Projected global average sea level rise during the 21st century and its components under SRES marker scenarios. The upper row in each pair gives the 5 to 95% range (m) of the rise in sea level between 1980 to 1999 and 2090 to 2099. The lower row in each pair gives the range of the rate of sea level rise (mm yr^{-1}) during 2090 to 2099. The land ice sum comprises G&IC and ice sheets, including dynamics, but excludes the scaled-up ice sheet discharge (see text). The sea level rise comprises thermal expansion and the land ice sum. Note that for each scenario the lower/upper bound for sea level rise is larger/smaller than the total of the lower/upper bounds of the contributions, since the uncertainties of the contributions are largely independent. See Appendix 10.A for methods.*

		B1		B2		A1B		A1T		A2		A1FI	
Thermal expansion	m	0.10	0.24	0.12	0.28	0.13	0.32	0.12	0.30	0.14	0.35	0.17	0.41
	mm yr^{-1}	1.1	2.6	1.6	4.0	1.7	4.2	1.3	3.2	2.6	6.3	2.8	6.8
G&IC	m	0.07	0.14	0.07	0.15	0.08	0.15	0.08	0.15	0.08	0.16	0.08	0.17
	mm yr^{-1}	0.5	1.3	0.5	1.5	0.6	1.6	0.5	1.4	0.6	1.9	0.7	2.0
Greenland Ice Sheet SMB	m	0.01	0.05	0.01	0.06	0.01	0.08	0.01	0.07	0.01	0.08	0.02	0.12
	mm yr^{-1}	0.2	1.0	0.2	1.5	0.3	1.9	0.2	1.5	0.3	2.8	0.4	3.9
Antarctic Ice Sheet SMB	m	-0.10	-0.02	-0.11	-0.02	-0.12	-0.02	-0.12	-0.02	-0.12	-0.03	-0.14	-0.03
	mm yr^{-1}	-1.4	-0.3	-1.7	-0.3	-1.9	-0.4	-1.7	-0.3	-2.3	-0.4	-2.7	-0.5
Land ice sum	m	0.04	0.18	0.04	0.19	0.04	0.20	0.04	0.20	0.04	0.20	0.04	0.23
	mm yr^{-1}	0.0	1.8	-0.1	2.2	-0.2	2.5	-0.1	2.1	-0.4	3.2	-0.8	4.0
Sea level rise	m	0.18	0.38	0.20	0.43	0.21	0.48	0.20	0.45	0.23	0.51	0.26	0.59
	mm yr^{-1}	1.5	3.9	2.1	5.6	2.1	6.0	1.7	4.7	3.0	8.5	3.0	9.7
Scaled-up ice sheet discharge	m	0.00	0.09	0.00	0.11	-0.01	0.13	-0.01	0.13	-0.01	0.13	-0.01	0.17
	mm yr^{-1}	0.0	1.7	0.0	2.3	0.0	2.6	0.0	2.3	-0.1	3.2	-0.1	3.9

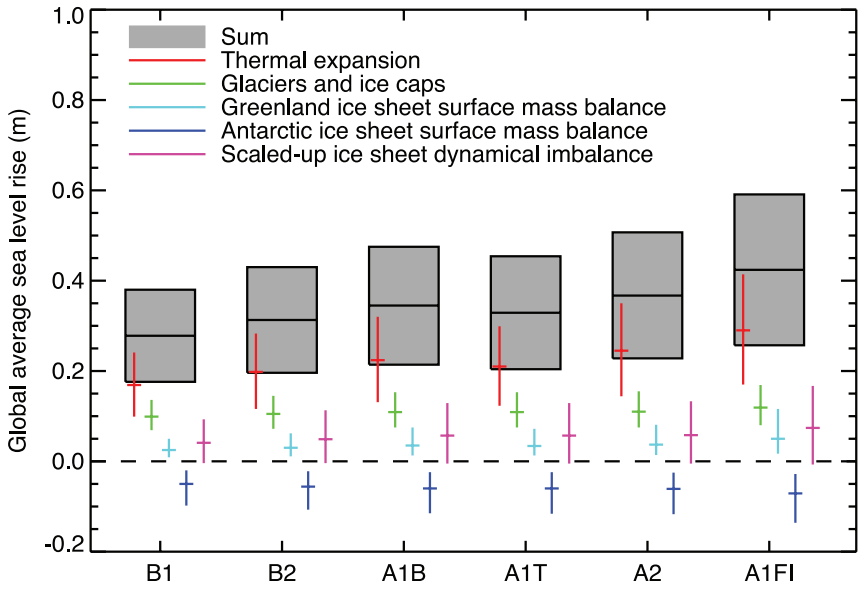

Figure 10.33. *Projections and uncertainties (5 to 95% ranges) of global average sea level rise and its components in 2090 to 2099 (relative to 1980 to 1999) for the six SRES marker scenarios. The projected sea level rise assumes that the part of the present-day ice sheet mass imbalance that is due to recent ice flow acceleration will persist unchanged. It does not include the contribution shown from scaled-up ice sheet discharge, which is an alternative possibility. It is also possible that the present imbalance might be transient, in which case the projected sea level rise is reduced by 0.02 m. It must be emphasized that we cannot assess the likelihood of any of these three alternatives, which are presented as illustrative. The state of understanding prevents a best estimate from being made.*

In all scenarios, the average rate of rise during the 21st century is very likely to exceed the 1961 to 2003 average rate of 1.8 ± 0.5 mm yr^{-1} (see Section 5.5.2.1). The central estimate of the rate of sea level rise during 2090 to 2099 is 3.8 mm yr^{-1} under A1B, which exceeds the central estimate of 3.1 mm yr^{-1} for 1993 to 2003 (see Section 5.5.2.2). The 1993 to 2003 rate may have a contribution of about 1 mm yr^{-1} from internally generated or naturally forced decadal variability (see Sections 5.5.2.4 and 9.5.2). These sources of variability are not predictable and not included in the projections; the actual rate during any future decade might therefore be more or less than the projected rate by a similar amount. Although simulated and observed sea level rise agree reasonably well for 1993 to 2003, the observed rise for 1961 to 2003 is not satisfactorily explained (Section 9.5.2), as the sum of observationally estimated components is 0.7 ± 0.7 mm yr^{-1} less than the observed rate of rise (Section 5.5.6). This indicates a deficiency in current scientific understanding of sea level change and may imply an underestimate in projections.

For an average model (the central estimate for each scenario), the scenario spread (from B1 to A1FI) in sea level rise is only 0.02 m by the middle of the century. This is small because of the time-integrating effect of sea level rise, on which the divergence among the scenarios has had little effect by then. By 2090 to 2099 it is 0.15 m.

In all scenarios, the central estimate for thermal expansion by the end of the century is 70 to 75% of the central estimate for the sea level rise. In all scenarios, the average rate of expansion during the 21st century is larger than central estimate of 1.6 mm yr^{-1} for 1993 to 2003 (Section 5.5.3). Likewise, in all scenarios the average rate of mass loss by G&IC during the 21st century is greater than the central estimate of 0.77 mm yr^{-1} for 1993 to 2003 (Section 4.5.2). By the end of the century, a large fraction of the present global G&IC mass is projected to have been lost (see, e.g., Table 4.3). The G&IC projections are rather insensitive to the scenario because the main uncertainties come from the G&IC model.

Further accelerations in ice flow of the kind recently observed in some Greenland outlet glaciers and West Antarctic ice streams could increase the ice sheet contributions substantially, but quantitative projections cannot be made with confidence (see Section 10.6.4.2). The land ice sum in Table 10.7 includes the effect of dynamical changes in the ice sheets that can be simulated with a continental ice sheet model (Section 10.6.4.2). It also includes a scenario-independent term of 0.32 ± 0.35 mm yr^{-1} (0.035 ± 0.039 m in 110 years). This is the central estimate for 1993 to 2003 of the sea level contribution from the Antarctic Ice Sheet, plus half of that from Greenland (Sections 4.6.2.2 and 5.5.5.2). We take this as an estimate of the part of the present ice sheet mass imbalance that is due to recent ice flow acceleration (Section 4.6.3.2), and assume that this contribution will persist unchanged.

We also evaluate the contribution of rapid dynamical changes under two alternative assumptions (see, e.g., Alley et al., 2005b). First, the present imbalance might be a rapid short-term adjustment, which will diminish during coming decades. We take an e-folding time of 100 years, on the basis of an idealised model study (Payne et al., 2004). This assumption reduces the sea level rise in Table 10.7 by 0.02 m. Second, the present imbalance might be a response to recent climate change, perhaps through oceanic or surface warming (Section 10.6.4.2). No models are available for such a link, so we assume that the imbalance might scale up with global average surface temperature change, which we take as a measure of the magnitude of climate change (see Appendix 10.A). This assumption adds 0.1 to 0.2 m to the estimated upper bound for sea level rise depending on the scenario (Table 10.7). During 2090 to 2099, the rate of scaled-up antarctic discharge roughly balances the increased rate of antarctic accumulation (SMB). The central estimate for the increased antarctic discharge under the SRES scenario A1FI is about 1.3 mm yr^{-1}, a factor of 5 to 10 greater than in recent years, and similar to the order-of-magnitude upper limit of Section 10.6.4.2. It must be emphasized that we cannot assess the likelihood of any of these three alternatives, which are presented as illustrative. The state of understanding prevents a best estimate from being made.

The central estimates for sea level rise in Table 10.7 are smaller than the TAR model means (Church et al., 2001) by 0.03 to 0.07 m, depending on scenario, for two reasons. First, these projections are for 2090-2099, whereas the TAR projections were for 2100. Second, the TAR included some small constant additional contributions to sea level rise which are omitted here (see below regarding permafrost). If the TAR model means are adjusted for this, they are within 10% of the central estimates from Table 10.7. (See Appendix 10.A for further information.) For each scenario, the upper bound of sea level rise in Table 10.7 is smaller than in the TAR, and the lower bound is larger than in the TAR. This is because the uncertainty on the sea level projection has been reduced, for a combination of reasons (see Appendix 10.A for details). The TAR would have had similar ranges to those shown here if it had treated the uncertainties in the same way.

Thawing of permafrost is projected to contribute about 5 mm during the 21st century under the SRES scenario A2 (calculated from Lawrence and Slater, 2005). The mass of the ocean will also be changed by climatically driven alteration in other water storage, in the forms of atmospheric water vapour, seasonal snow cover, soil moisture, groundwater, lakes and rivers. All of these are expected to be relatively small terms, but there may be substantial contributions from anthropogenic change in terrestrial water storage, through extraction from aquifers and impounding in reservoirs (see Sections 5.5.5.3 and 5.5.5.4).

10.7 Long Term Climate Change and Commitment

10.7.1 Climate Change Commitment to Year 2300 Based on AOGCMs

Building on Wigley (2005), we use three specific definitions of climate change commitment: (i) the 'constant composition commitment', which denotes the further change of temperature ('constant composition temperature commitment' or 'committed warming'), sea level ('constant composition sea level commitment') or any other quantity in the climate system, since the time the composition of the atmosphere, and hence the radiative forcing, has been held at a constant value; (ii) the 'constant emission commitment', which denotes the further change of, for example, temperature ('constant emission temperature commitment') since the time the greenhouse gas emissions have been held at a constant value; and (iii) the 'zero emission commitment', which denotes the further change of, for example, temperature ('zero emission temperature commitment') since the time the greenhouse gas emissions have been set to zero.

The concept that the climate system exhibits commitment when radiative forcing has changed is mainly due to the thermal inertia of the oceans, and was discussed independently by Wigley (1984), Hansen et al. (1984) and Siegenthaler and Oeschger (1984). The term 'commitment' in this regard was introduced by Ramanathan (1988). In the TAR, this was illustrated in idealised scenarios of doubling and quadrupling atmospheric CO_2, and stabilisation at 2050 and 2100 after an IS92a forcing scenario. Various temperature commitment values were reported (about 0.3°C per century with much model dependency), and EMIC simulations were used to illustrate the long-term influence of the ocean owing to long mixing times and the MOC. Subsequent studies have confirmed this behaviour of the climate system and ascribed it to the inherent property of the climate system that the thermal inertia of the ocean introduces a lag to the warming of the climate system after concentrations of greenhouse gases are stabilised (Mitchell et al., 2000; Wetherald et al., 2001; Wigley and Raper, 2003; Hansen et al., 2005b; Meehl et al., 2005c; Wigley, 2005). Climate change commitment as discussed here should not be confused with 'unavoidable climate change' over the next half century, which would surely be greater because forcing cannot be instantly stabilised. Furthermore, in the very long term it is plausible that climate change could be less than in a commitment run since forcing could plausibly be reduced below current levels as illustrated in the overshoot simulations and zero emission commitment simulations discussed below.

Three constant composition commitment experiments have recently been performed by the global coupled climate modelling community: (1) stabilising concentrations of greenhouse gases at year 2000 values after a 20th-century climate simulation, and running the model for an additional 100 years; (2) stabilising concentrations of greenhouse gases at year 2100 values after a 21st-century B1 experiment (e.g., CO_2 near 550 ppm) and running the model for an additional 100 years (with some models run to 200 years); and (3) stabilising concentrations of greenhouse gases at year 2100 values after a 21st-century A1B experiment (e.g., CO_2 near 700 ppm), and running the model for an additional 100 years (and some models to 200 years). Multi-model mean warming in these experiments is depicted in Figure 10.4. Time series of the globally averaged surface temperature and percent precipitation change after stabilisation are shown for all the models in the Supplementary Material, Figure S10.3.

The multi-model average warming for all radiative forcing agents held constant at year 2000 (reported earlier for several of the models by Meehl et al., 2005c), is about 0.6°C for the period 2090 to 2099 relative to the 1980 to 1999 reference period. This is roughly the magnitude of warming simulated in the 20th century. Applying the same uncertainty assessment as for the SRES scenarios in Fig. 10.29 (–40 to +60%), the likely uncertainty range is 0.3°C to 0.9°C. Hansen et al. (2005a) calculate the current energy imbalance of the Earth to be 0.85 W m^{-2}, implying that the unrealised global warming is about 0.6°C without any further increase in radiative forcing. The committed warming trend values show a rate of warming averaged over the first two decades of the 21st century of about 0.1°C per decade, due mainly to the slow response of the oceans. About twice as much warming (0.2°C per decade) would be expected if emissions are within the range of the SRES scenarios.